Rapidity Dependence of Charged Particle Yields for Au+Au at $\sqrt{s_{NN}} = 200\,\text{GeV}$

Djamel Ouerdane[a] for the BRAHMS Collaboration

[a]Niels Bohr Institute, Blegdamsvej 17
2100 Copenhagen Ø, Denmark

Yields of charged particles ($\pi^\pm$, $K^\pm$, p and $\bar{p}$) have been derived from spectra measured with BRAHMS for the reaction Au+Au at $\sqrt{s_{NN}} = 200\,\text{GeV}$, as a function of rapidity in the range $y = 0$ to $y \approx 3$ for the 10% most central events. The yields peak at mid-rapidity with a small decrease in the range $|y| \lesssim 1$ but they drop significantly at higher rapidities except for the protons. At $y = 0$, the K^-/π^- ratio is 0.18 ± 0.02 (syst), very close to the K^+/π^+ ratio equal to 0.19 ± 0.02 (syst). but at $y = 3$, K^-/π^- drops to 0.12 ± 0.02 (syst) while K^+/π^+ remains constant.

1. INTRODUCTION

In 2001, the Relativistic Heavy Ion Collider (RHIC) provided gold beams at the full design energy ($\sqrt{s_{NN}} = 200\,\text{GeV}$). The BRAHMS experiment made a unique set of measurements of charged hadrons over a wide range of rapidity ($y = 0$ to $y \approx 3.5$). We present here for the first time the rapidity dependence of hadronic yields for the 10% most central events for the reaction Au + Au at $\sqrt{s_{NN}} = 200\,\text{GeV}$. The BRAHMS detector system consists of two independent and movable spectrometers (MRS and FS) and a set of detectors for reaction characterization (centrality and interaction point). The ability to rotate the spectrometers added to the use of different magnetic field settings allows the exploration of a large fraction of the full phase-space, as illustrated in Fig. 1 for pions. For the work reported here, the MRS was operated at 90, 45 and 40 degrees, and the FS
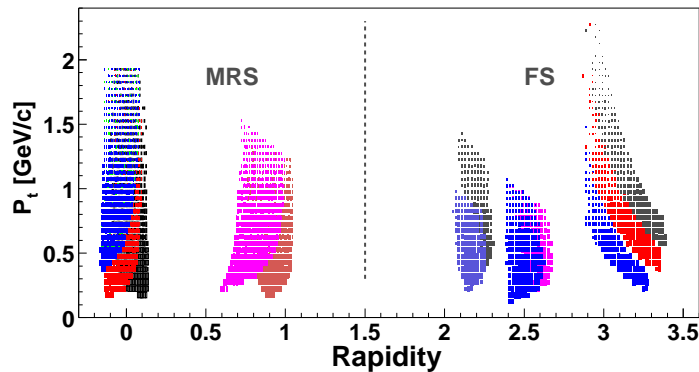

Figure 1. Pion acceptance. Only the data used for this analysis is shown.

at 3, 4, 8 and 12 degrees. More details about the experimental setup can be found in [1, 2].

2. CHARGED PARTICLE SPECTRA

Since the BRAHMS spectrometers subtend a small solid angle, charged particle spectra are constructed by combining several data sets measured at different angles relative to the beam line with various magnetic fields. For each setting, acceptance correction maps $(p_t$ or $m_t, y)$ are built for each particle specie, by using a Monte-Carlo calculation based on GEANT3, simulating the particle tracking through the BRAHMS detector system. Corrections for detector efficiency, absorption and particle decay are then applied to p_t or m_t spectra. Figure 2 shows normalized particle spectra for $\pi^\pm$, $K^\pm$, p and $\bar{p}$ at $y = 0$ (top) and $y \approx 3$ (bottom). At mid-rapidity, positive and negative spectra have similar slopes
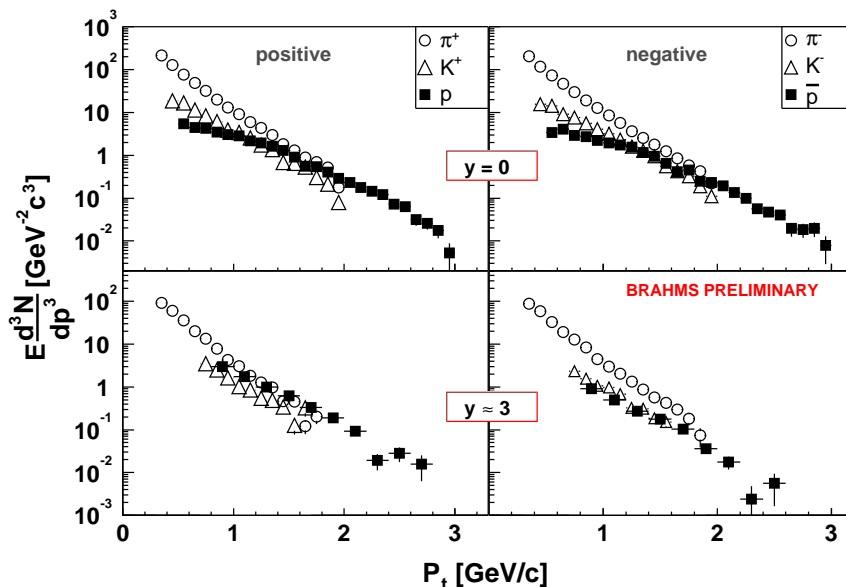

Figure 2. Transverse momentum distributions of $\pi^\pm$, $K^\pm$, p and $\bar{p}$ at $y = 0$ (top) and $y \approx 3$ (bottom) for the top 10% most central reactions. Positive (negative) particle spectra are shown on the left (right) panels.

and magnitudes. The inverse slopes increase with the mass of the particles, and for the proton and anti-proton, the spectra reach and exceed the pion yields at $p_t \approx 2\,\text{GeV/c}$, as was observed at $\sqrt{s_{NN}} = 130\,\text{GeV}$ [3]. At $y \approx 3$, yields differ between K^+ and K^- as well as between p and $\bar{p}$ although slopes are similar (cf. table 1).

3. RAPIDITY DENSITY

Rapidity densities were evaluated by fitting the particle spectra with an exponential function $\propto exp\left[-(m_t - m)/T\right]$ which was then integrated. Statistical errors are between 1% and 4%, whereas systematics errors are estimated to be 15% at mid-rapidity and 20% at the highest rapidity investigated for this analysis. These errors come from various sources. One is the extrapolation of the lower part of the p_t spectra. The MRS acceptance

covers 65% of the of the total spectrum range for pions, 60% for kaons and 70% for the protons, while the FS acceptance covers around 50% for pions, 30% for kaons and 60% for protons. Another main source is the use of different data sets where background conditions can differ. The results are summarized in table 1 and the rapidity density of charged hadrons is shown in Fig. 3. The measured densities fall off by $\simeq 20\%$ in the range
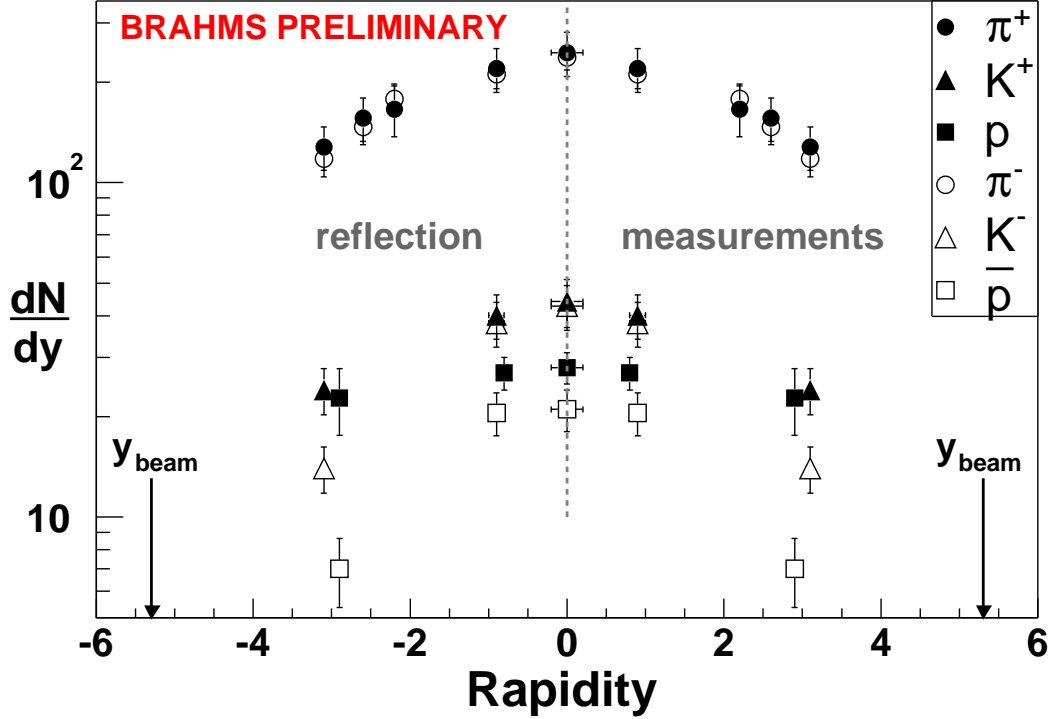

Figure 3. Rapidity density versus rapidity for $\pi^{\pm}$, $K^{\pm}$, p and $\bar{p}$. The data has been reflected about $y = 0$.

$|y| \lesssim 1$. We also note that the density ratios between matter and antimatter are close to unity, as was already observed in [12]. As we go towards higher rapidities, all particle densities show a significant drop except for the protons (yields were not corrected for hyperon decays). While π^+ and π^- yields decrease evenly, K^- yields drop faster than K^+ yields. This is illustrated in Fig. 4, which shows the K/π ratios as a function of $\sqrt{s_{NN}}$. We note that the K^-/π^- at midrapidity increases monotonically to 0.18 ± 0.02 (syst) as $\sqrt{s_{NN}}$ increases. In contrast, the K^+/π^+ evolution seems to show a saturation of the positive strangeness from $\sqrt{s_{NN}} = 17\,\text{GeV}$ to $200\,\text{GeV}$ where it is equal to 0.19 ± 0.02 (syst), which is comparable with the mid-rapidity results from central Pb + Pb reactions at SPS [10]. At this particular energy, no rapidity dependence was observed for K^+/π^+ but the K^-/π^- ratio drops to 0.12 ± 0.02 (syst) at $y \approx 3$. At this rapidity, the ratios are comparable with the results from [8]. This behaviour at the highest RHIC energy appears to be consistent with the rapidity dependence of the proton and antiproton yields detailed in [13].
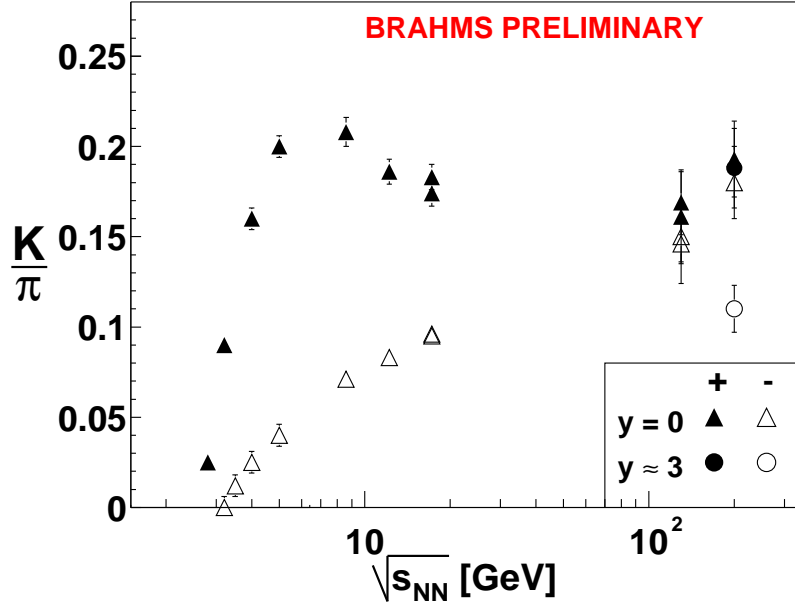
Figure 4. Kaon to pion ratio as a function of $\sqrt{s_{NN}}$. Data below $\sqrt{s_{NN}} = 5\,\text{GeV}$ are from [4, 5, 6, 7], data between $5\,\text{GeV}$ and $20\,\text{GeV}$ from [8, 9, 10], and at $130\,\text{GeV}$ from [3, 11]

4. SUMMARY

The particle densities of produced charged hadrons exhibit a significant variation with rapidity, that is consistent with a gaussian distribution with a full width of $\simeq 6$ units in rapidity for pions. The inverse slopes decrease with increasing rapidity for pions, kaons and protons but differences between particle species still remain at y ≈ 3. This indicates that radial flow is still present at these high rapidities. The strangeness production is also strongly dependent on rapidity. It is shown that K^+ and K^- are produced in almost equal amounts at mid-rapidity. As $y \approx 3$ though, we notice that the K^-/π^- ratio is about 60% of the K^+/π^+ ratio, which reflects the decreasing importance of the pair production mechanism with increasing rapidity[1].

Table 1
Inverse slope parameters and rapidity densities for $\pi^{\pm}$ and $K^{\pm}$. Only statistical errors are given.

y	T_{π^+}	N_{π^+}	T_{π^-}	N_{π^-}	T_{K^+}	N_{K^+}	T_{K^-}	N_{K^-}
0	224 ± 4	245 ± 3	221 ± 2	237 ± 3	283 ± 6	47 ± 2	294 ± 6	43 ± 1
0.8	-	-	-	-	293 ± 11	40 ± 1	294 ± 10	38 ± 1
0.9	219 ± 3	216 ± 2	216 ± 2	211 ± 2	-	-	-	-
2.2	205 ± 3	166 ± 3	205 ± 2	178 ± 3	-	-	-	-
2.6	199 ± 3	156 ± 2	186 ± 3	147 ± 3	-	-	-	-
3.1	199 ± 2	128 ± 2	208 ± 3	118 ± 3	246 ± 12	24 ± 1	263 ± 12	14 ± 1

[1]See [13] for a discussion about baryon stopping.

REFERENCES

1. M. Adamczyk *et al* [BRAHMS Collaboration], submitted to Nucl. Inst. Meth. (2002).
2. I. G. Bearden *et al* [BRAHMS Collaboration], these proceedings.
3. K. Adcox *et al* [PHENIX Collaboration], Phys. Rev. Lett. **88** (2002), 242301.
4. L. Ahle *et al* [E802 Collaboration], Phys. Rev. **C57** (1998) 466.
5. L. Ahle *et al* [E802 Collaboration], Phys. Rev. **C58** (1998) 3523.
6. L. Ahle *et al* [E866 and E917 Collaboration], Phys. Lett. **B** 476 (2000) 1.
7. L. Ahle *et al* [E866 and E917 Collaboration], Phys. Lett. **B** 490 (2000) 53.
8. S. V. Afanasiev *et al* [NA49 Collaboration], Nucl. Phys. A 698 (2002) 104c.
9. S. V. Afanasiev *et al* [NA49 Collaboration], nucl-ex/0205002.
10. I. G. Bearden *et al* [NA44 Collaboration], nucl-ex/0202019.
11. C. Adler *et al* [STAR Collaboration], nucl-ex/0206008.
12. I. G. Bearden *et al* [BRAHMS Collaboration], nucl-ex/0207006.
13. J. H. Lee *et al* [BRAHMS Collaboration], these proceedings.